



Climate change scenarios for global impacts studies

Mike Hulme^{a,*}, John Mitchell^b, William Ingram^b, Jason Lowe^b, Tim Johns^b, Mark New^a, David Viner^a

^aClimatic Research Unit, School of Environmental Sciences, UEA, Norwich, UK

^bHadley Centre for Climate Prediction and Research, UK Met. Office, London Road, Bracknell, UK

Received 21 May 1999

Abstract

We describe a set of global climate change scenarios that have been used in a series of studies investigating the global impacts of climate change on several environmental systems and resources — ecosystems, food security, water resources, malaria and coastal flooding. These scenarios derive from modelling experiments completed by the Hadley Centre over the last four years using successive versions of their coupled ocean-atmosphere global climate model. The scenarios benefit from ensemble simulations (made using HadCM2) and from an un-flux-corrected experiment (made using HadCM3), but consider only the effects of increasing greenhouse gas concentrations. The effects of associated changes in sulphate aerosol concentrations are not considered. The scenarios are presented for three future time periods — 30-year means centred on the 2020s, the 2050s and the 2080s — and are expressed with respect to the mean 1961–1990 climate. A global land observed climatology at 0.5° latitude/longitude resolution is used to describe current climate. Other scenario variables — atmospheric CO₂ concentrations, global-mean sea-level rise and non-climatic assumptions relating to population and economy — are also provided. We discuss the limitations of the created scenarios and in particular draw attention to sources of uncertainty that we have not fully sampled. © 1999 Elsevier Science Ltd. All rights reserved.

Keywords: Climate change scenarios; HadCM2; HadCM3; Sea-level rise

1. Introduction

Assessments of the possible impacts of future climate change require descriptions on appropriate space and time-scales of possible future climates. These descriptions, or scenarios, most commonly originate from climate change experiments made using global climate models (GCMs). The history of using GCM results for impacts assessments extends over about 15 years or more with some of the earliest examples being described in Santer (1985), Rosenzweig (1985) and Emanuel et al. (1985). Parry and Carter (1998) provide an overview of how climate change scenarios may be constructed and applied in impacts assessments, while Hulme and Carter (1999) provide a systematic assessment of the various sources of uncertainties in these types of studies. These

uncertainties include those arising from different forcing scenarios (e.g. Nakicenovic et al., 1998), from climate model differences (e.g. Kittel et al., 1998), and from climate system unpredictability (e.g. Mitchell et al., 1999; Giorgi and Francisco, 1999). It is rare for impacts assessments to sample these uncertainties comprehensively (Hulme and Carter, 1999), although a full risk assessment of climate change impact requires such a comprehensive approach.

In the global climate scenarios reported in this study, we sample only a single future forcing scenario (~1% per annum growth in greenhouse gas concentrations) and use results from only one modelling centre, the Hadley Centre at the UK Met. Office. We do, however, construct scenarios using results from two different versions of the Hadley Centre GCM (HadCM2 and HadCM3) and we also examine the effect of ensemble simulations on the resulting scenarios.

This paper therefore describes the climate and related scenarios that were used in the various global impacts assessments that are reported in this Special Issue of

* Corresponding author.

E-mail address: m.hulme@uea.ac.uk (M. Hulme)

Global Environmental Change. These assessments covered impacts of climate change on ecosystems and the terrestrial carbon sink (White et al., 1999), food security (Parry et al., 1999), water resources (Arnell, 1999), malaria distribution (Martens et al., 1999) and coastal flooding (Nicholls et al., 1999). Section 2 summarises the observed baseline climatology that was used in the impacts assessments, while Section 3 describes the two climate models, HadCM2 and HadCM3, that were used to conduct the experiments that formed the basis of the climate change scenarios. Any model simulation of future anthropogenic climate change requires a forcing scenario to be specified and Section 4 explains the forcing scenarios used in the HadCM2 and HadCM3 experiments. Some of the salient features of the model-simulated future climates are described in Section 5, focusing on those surface climate variables and time-periods that were used in the subsequent impacts assessments. In Section 6, we describe how we have combined the observed and modelled data to create the climate scenarios used in the impacts studies. Some of the other, non-climatic, scenario variables required for impacts assessments are discussed in Section 7 and we justify the choices we have made in this study. Finally, Section 8 discusses some of the uncertainties associated with the type of climate change scenario constructed here, uncertainties related both to the forcing scenario adopted and to the global climate model used in the simulation.

2. The observed global climatology

To undertake climate change impacts assessments at a global scale requires an appropriate global observed climate data set describing current climate conditions. For this purpose we used the newly created mean monthly terrestrial climate data set of New et al. (1999a). This data set has been created specifically to support the sorts of climate change impacts assessments described in this Special Issue. It exists at a spatial resolution of 0.5° latitude/longitude resolution for all global land areas (excluding Antarctica) and for the following surface climate variables at monthly resolution: mean air temperature, diurnal temperature range, precipitation total, vapour pressure, total cloud cover, wind speed (15 m estimate), wet day frequency (< 0.1 mm), and ground frost frequency. All of these variables, with the exception of ground frost frequency, are used in one or more of the reported impacts studies (see New et al., 1999a for more details). These mean monthly values describe mean climate conditions over the standard WMO normal period 1961–1990 (yearly anomalies from this mean climatology for the period 1901–1995 have also been created; New et al., 1999b, but are not used here). For illustrative purposes, we display three global fields from this 1961–1990 climatology in Fig. 1.

3. The HadCM2 and HadCM3 climate models

3.1. HadCM2

The second generation Hadley Centre coupled model (HadCM2) has a horizontal resolution of 2.5° in latitude by 3.75° in longitude. This gives a grid spacing of 278 km in the North–South direction and 417 km East–West at the Equator reducing to 295 km at 45° North and South (comparable to a T42 spectral model resolution). There are 19 levels in the model atmosphere and 20 levels in the model ocean.

There is a detailed treatment of shortwave (Slingo, 1989) and longwave radiation (Slingo and Wilderspin, 1986) including the full diurnal and annual cycles. Over land, albedo is computed from snow-free and deep snow albedos, specified according to vegetation type and based on predicted snow depth and surface air temperature. A parametrization of orographic gravity waves is included (Palmer et al., 1986).

Surface fluxes are a function of atmospheric stability (Smith, 1990) and climatological surface-type layers. A four-layer soil temperature model (Warrilow et al., 1986) is embedded in the land surface scheme. Surface hydrology calculations take account of storage of water in a vegetative canopy in addition to ground storage. Canopy evaporation and transpiration, throughfall of moisture from the canopy to the ground, and surface and sub-surface runoff are all modelled based on Warrilow et al. (1986). In calculating canopy throughfall and surface runoff, a distribution of rainfall rate within each gridbox is assumed (Dolman and Gregory, 1992). River runoff is included in the model using pre-defined river catchments. The runoff enters the ocean at coastal outflow points that are defined on the ocean model grid. There is no explicit river transport in the model, so runoff is transported instantaneously to the ocean. Convective rainfall and snowfall are calculated using a mass flux penetrative convection scheme (Gregory and Rowntree, 1990), with the addition of an explicit downdraught representation (Gregory and Allen, 1991). Large-scale (dynamic) rainfall and snowfall calculations are based on cloud water and ice contents (Smith, 1990).

The ocean component of the model is based on the Bryan–Cox primitive equation model (Bryan, 1969a; Cox, 1984). The level spacing is small near the surface in order to resolve the mixed layer, the top layer being 10 m thick. Bottom topography is derived from the Scripps one degree resolution orography data set (Gates and Nelson, 1973), with single gridpoint inlets and basins removed. An energy balance mixed-layer model based on Kraus and Turner (1967) is embedded in the model. Further vertical mixing is provided at all depths. A horizontal momentum diffusivity (eddy viscosity) is applied. The mixing of temperature and salinity across the Straits of Gibraltar is parameterized.

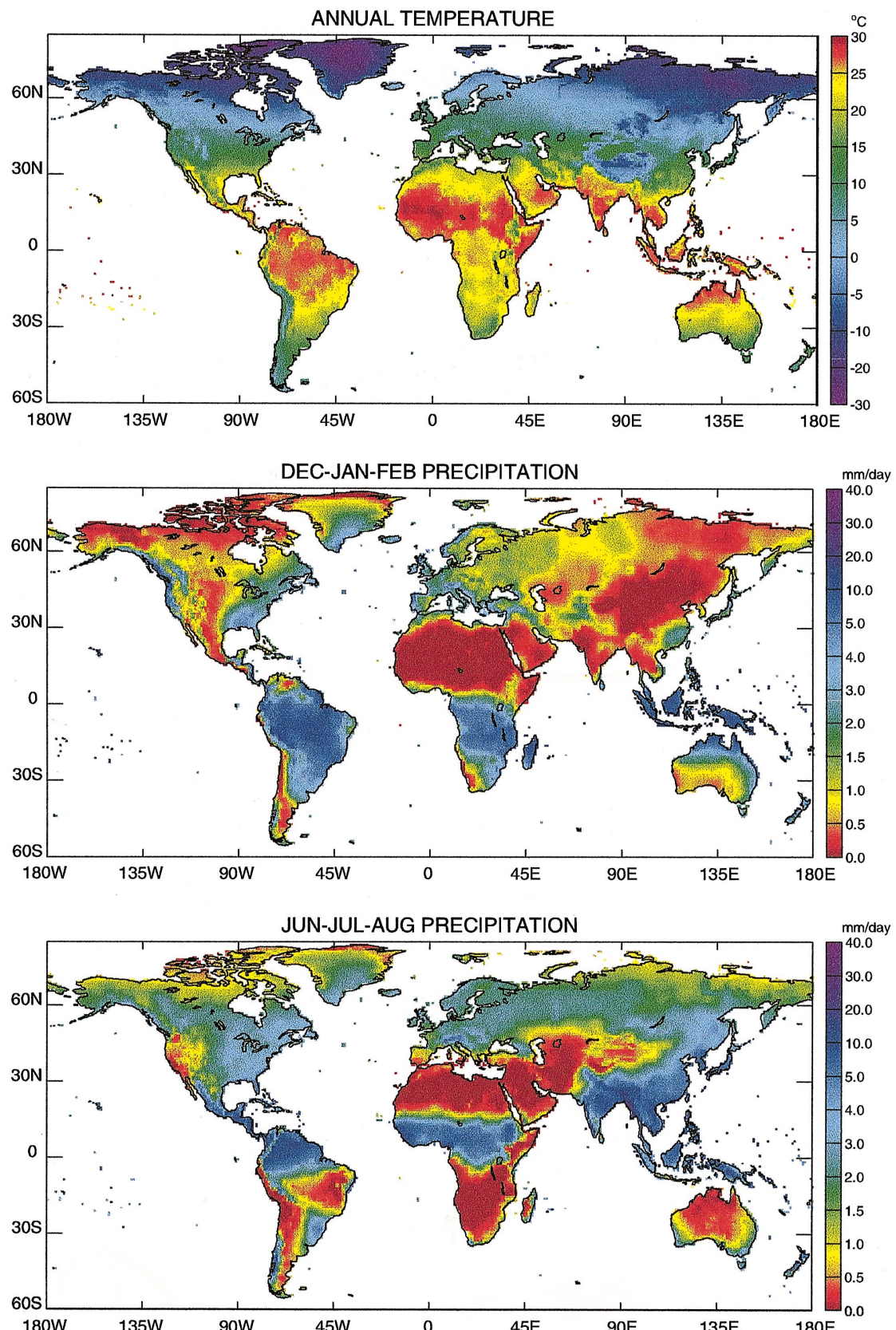


Fig. 1. Observed global land mean climate fields for 1961–1990 extracted from the New et al. (1999a) data set; (top) annual mean temperature ($^{\circ}\text{C}$); (middle) boreal winter (DJF) mean precipitation rate (mm d^{-1}); (bottom) boreal summer (JJA) mean precipitation rate (mm d^{-1}).

The sea-ice component is a ‘zero-layer’ model sharing the ocean model horizontal grid, but with the addition of simple ice and snow advection (Bryan, 1969b). The thermodynamics of the model is based on the zero-layer model of Semtner (1976). A parameterisation of ice concentration based on that of Hibler (1979) is included. Surface fluxes over the ice and leads fractions of each grid box, together with surface temperatures, are calculated separately within the atmosphere component of the model. An oceanic heat flux into the base of the ice is included. The coupling cycle consists of a one-day integration of the atmosphere model during which fluxes of heat, momentum, water and wind-mixing energy are averaged followed by a one-day integration of the ocean model. During the ocean cycle, averaged atmospheric fluxes are supplied from the preceding atmosphere cycle, with additional fluxes of heat and fresh water calculated to keep the ocean surface temperature (SST) and salinity (SSS) close to specified seasonally varying reference climatologies. Without these ‘flux adjustments’, the coupled model would rapidly drift away from a realistic state.

A fuller description of the model is given in Johns et al. (1997) and references therein. Various papers summarise the model’s simulation of precipitation (Airey et al., 1996), variability (Tett et al., 1997), storm tracks (Carnell and Senior, 1998) and response to anthropogenic forcing (Mitchell et al., 1995; Mitchell and Johns, 1997; Gregory and Mitchell, 1998; Mitchell et al., 1999). The effective climate sensitivity of the model over the next century is about 2.5°C for a doubling of atmospheric carbon dioxide concentration.

3.2. HadCM3

HadCM3 is an improved version of HadCM2 which does not use artificial fluxes of heat and moisture into the ocean to maintain a stable climate. The atmospheric resolution is the same as HadCM2, but the horizontal resolution over the ocean is 1.25° latitude by 1.25° longitude.

The new radiation scheme in HadCM3 allows the explicit representation of radiative effect of greenhouse gases and aerosols (Edwards and Slingo, 1996). A parameterisation of a simple background aerosol climatology (Cusack et al., 1998) is also included. The convection scheme has been improved by adding a parameterisation of the direct impact of convection on momentum (Gregory et al., 1997). A new land surface scheme (Cox et al., 1998) includes the representation of the freezing and melting of soil moisture and the formulation of evaporation includes the dependence of stomatal resistance on temperature, vapour pressure and CO₂. The parameterisation of orographic drag has been added (Milton and Wilson, 1996) and the gravity wave drag scheme has been extended (Gregory et al., 1998). A parameterisation

of the effective radius of cloud droplets as a function of cloud water content and droplet number concentration is also included (Martin et al., 1994). Several parameters in the layer cloud scheme have been altered compared to HadCM2 and there were some significant revisions to boundary layer mixing including the removal of a non-local mixing scheme (Smith, 1993). These and other minor changes are documented in Pope et al. (1999).

In addition to increasing the horizontal resolution, there are other significant changes to the ocean model. Horizontal mixing of tracers uses a version of the Gent and McWilliams (1990) adiabatic diffusion. The thickness diffusion coefficient formulation is determined locally (Visbeck et al., 1997). There is no explicit horizontal tracer diffusion in the model. The along-isopycnal diffusion coefficient is 1000 m² s⁻¹ and does not vary with depth. The increased horizontal resolution allows the use of a considerably smaller coefficient of horizontal momentum viscosity leading to an improved simulation of ocean currents. The convective adjustment is modified in the region of the Denmark Straits and Iceland–Scotland Ridge to better represent the down slope mixing of the overflow water based on the scheme used by Roether et al. (1994). The sea-ice model, which is the same as that used in HadCM2, uses a simple thermodynamic scheme and contains parameterisations of ice drift and leads (Cattle and Crossley, 1995).

Further details of the model are given in Gordon et al. (1999) and some initial climate changes experiments are described in Mitchell et al. (1998) and Wood et al. (1999). The equilibrium climate sensitivity of the model over the next century to doubling atmospheric CO₂ concentration is about 3.3°C, based on an experiment using HadCM3 with a mixed-layer ocean model (Senior, pers. comm.).

4. The GCM experiments

In the HadCM2 experiment, atmospheric CO₂ concentration was increased so as to give the radiative forcing due to observed greenhouse gases increases since pre-industrial times starting from 1860 up to the present day (1990), and then increased at 1% yr⁻¹ thereafter. The use of increases in CO₂ as a surrogate for the effect of other greenhouse gases is sometimes referred to as “equivalent CO₂”. We have also estimated what the increase in *actual* CO₂ concentration would be with respect to the observed 1990 CO₂ concentration of about 354 ppmv (Fig. 2). To do this, we assumed that the same fraction of the warming is due to increases in *actual* CO₂ as was assumed in the IS92a emissions scenario using the forcing-concentration relationships reported by the IPCC in 1992 (Mitchell and Gregory, 1992).

For HadCM2, an ensemble of four simulations was completed, each ensemble member starting from initial

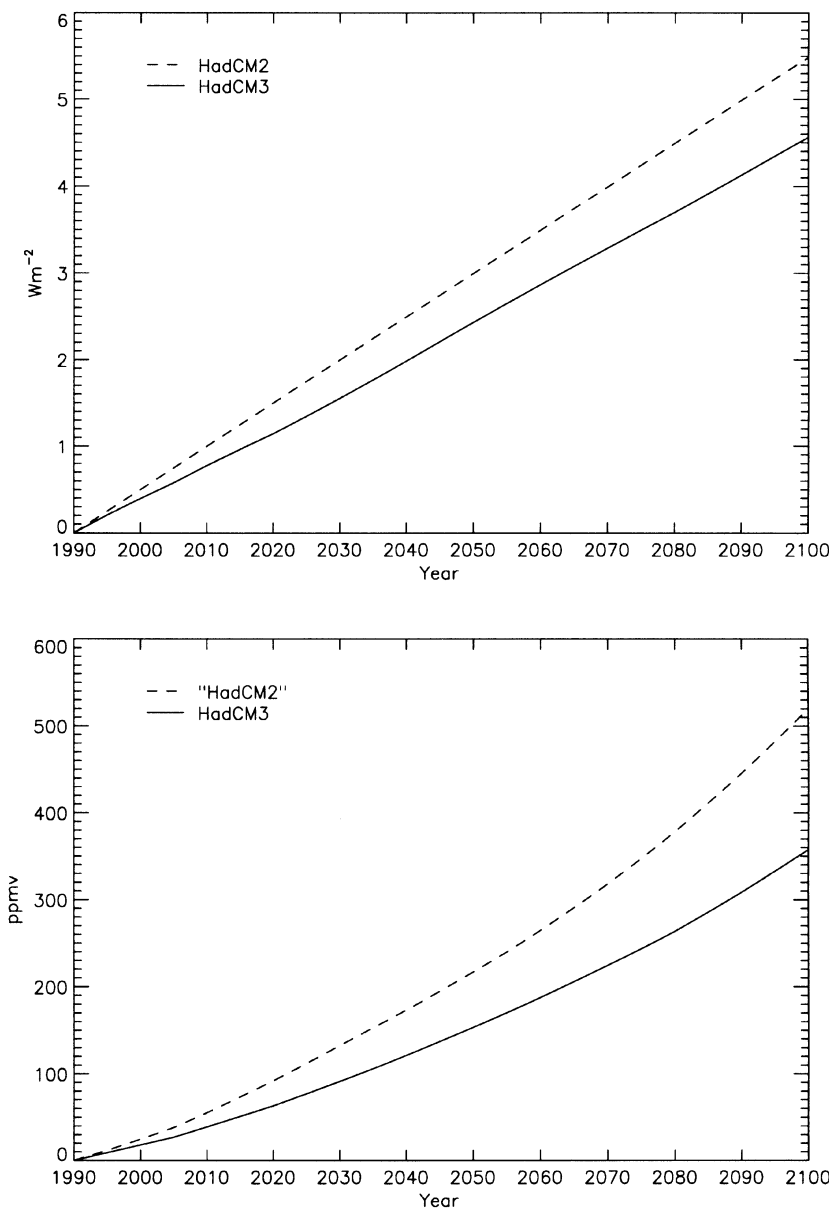


Fig. 2. (top) Changes in radiative heating at the tropopause (W m^{-2}) with respect to 1990, due to changes in greenhouse gases in HadCM2 (dashed curve) and HadCM3 (solid curve); (bottom) changes in CO_2 concentration (ppmv) as used in HadCM3 (solid curve). The dashed curve in the bottom panel shows the change in CO_2 which would give the same fractional contribution to radiative heating in the HadCM2 experiment as the increases in CO_2 gave in the HadCM3 experiment (see text).

conditions 100 years apart in the unforced control simulation. The use of slightly different initial conditions leads to different evolutions of climate change, due to the unpredictable nature of internal climate variability. This unpredictability arises from the chaotic nature of the model (and real) world. The spread of the changes in the ensemble gives an estimate of the range of changes expected with the given forcing scenario. Except where stated, ensemble-mean results are presented in this paper.

In HadCM3, greenhouse gas concentrations were increased from their 1860 values up to present (1990) as observed and then for 1990–2100 following the concen-

trations specified for the IS92a emissions scenario by Kattenberg et al. (1996). Note that the IPCC changed their concentration-forcing relationships between 1992 and 1996 and therefore although both HadCM2 and HadCM3 are forced by the same 1% yr increase in CO_2 -equivalent concentration, this translates into slightly different forcing scenarios. The increase in radiative forcing during the 21st century for HadCM3 is 1.0 W m^{-2} (about 20%) smaller than for HadCM2 by 2100 (Fig. 2). The ratio of the increases in CO_2 concentration (HadCM2/HadCM3) is much greater than the ratio of the changes in radiative heating. There is

a greater increase in heating in HadCM2, so a greater increase in CO₂ is required to produce the same fractional increase in heating as in HadCM3. Also, because the heating due to doubling CO₂ in HadCM2 is less than in HadCM3 (3.47 W m⁻² after allowing for stratospheric adjustment and solar absorption, compared to 3.74 W m⁻²), a larger increase in CO₂ is required to give the same change in heating. Note also that the increase in forcing varies as the logarithm of the change in CO₂ concentration. Only one simulation with HadCM3 was completed.

5. Patterns of climate change from the GCM experiments

5.1. Changes in temperature

The global-mean temperature response is very similar in both models. The slightly larger forcing in HadCM2 (Fig. 2) is largely offset by the lower climate sensitivity of this model (2.5°C) compared to HadCM3 (3.3°C). By 2100, and with respect to 1961–1990, there is a warming of about 2.5° and 5°C over sea and land, respectively (Fig. 3). The HadCM3 curves show greater interannual variability than HadCM2 since they are derived from only one simulation. The global-mean temperature increases

by about 0.3°C/decade, which is in good agreement with the IPCC “best guess” warming for the IS92a emissions scenario, ignoring aerosol effects (Kattenberg et al., 1996).

The patterns of temperature change (Figs. 4 and 5) show the characteristics common to other such experiments (for example, Kattenberg et al., 1996). Thus, the land warms more than the ocean (recall Fig. 3), the maximum warming occurs in the Arctic, the southern ocean warms only a little, especially in HadCM3, and there is a minimum warming in the northern North Atlantic, particularly in HadCM3. The main difference between the model responses is that HadCM2 warms more in the tropics and less in mid-latitudes than HadCM3. This is due to the differences in the representation of cloud and land surface processes in the two models (for example, Mitchell et al., 1998). By the end of the century, the warming in HadCM2 is 2°C greater over central Africa, but 1–2°C smaller over Western Europe, the United States and much of South America.

In HadCM2, the northern mid-latitude continents have warmed by over 1°C in the 2020s, 2° to 3°C by the 2050s and 3–4°C by the 2080s (Fig. 4). Similarly, there is a fairly uniform progression of warming in HadCM3, reaching over 5°C in the central northern continents by the 2080s (Fig. 5). The patterns of temperature change remain reasonably constant over time. For example, the

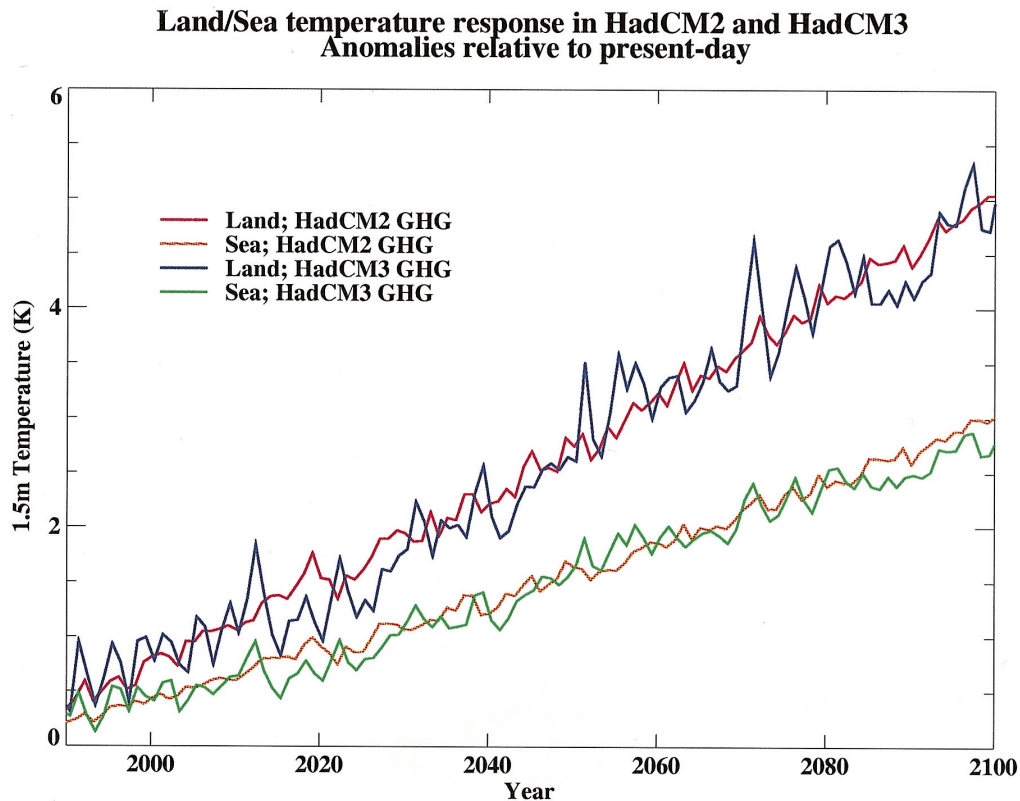


Fig. 3. Global-mean change with respect to 1961–1990 in surface air temperature over land (red curve, HadCM2; blue curve, HadCM3) and ocean (yellow curve, HadCM2; green curve HadCM3).

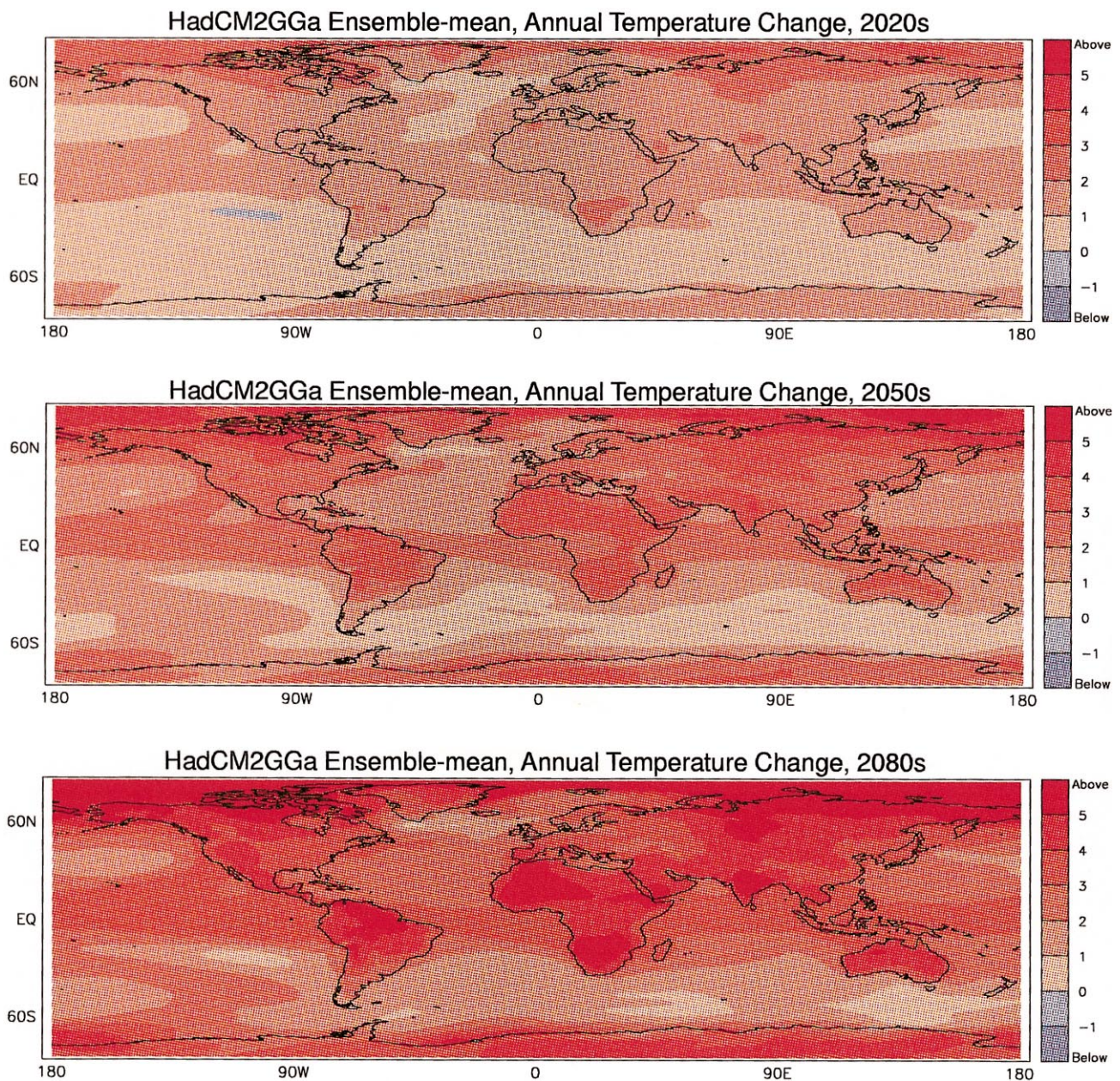


Fig. 4. Annual mean surface air temperature change (degC) with respect to 1961–1990 for the 2020s (top), 2050s (middle) and 2080s (bottom); HadCM2 ensemble-mean. The three periods are averaged over 30-years centred on the above decades.

maxima in warming over South America, southern Africa and central and northeastern Asia in HadCM3 at the end of the next century (Fig. 5, bottom) are also evident near the beginning and middle of the century (Fig. 5, top and middle, respectively). A more detailed analysis confirming the approximate constancy of the patterns of change in HadCM2 is given in Mitchell et al. (1999).

5.2. Changes in cloud cover

In HadCM2, cloud cover increases predominate in the southern extra-tropics and northern high latitudes

(Fig. 6, top). Elsewhere, cloud cover generally decreases, the main exceptions being bands of increase in low latitudes of the Pacific and southern Atlantic Oceans which extend eastwards and polewards into mid-latitudes. For example, there is an increase in cloud cover in the north-eastern Pacific stretching into North America. There are also increases in cloud cover over North Africa. Note that increases in precipitation do not necessarily lead to increases in cloud, particularly in low latitudes. For example, the increases in precipitation extending eastwards from the Philippines (Fig. 7) coincide with decreases in cloud cover (Fig. 6, top).

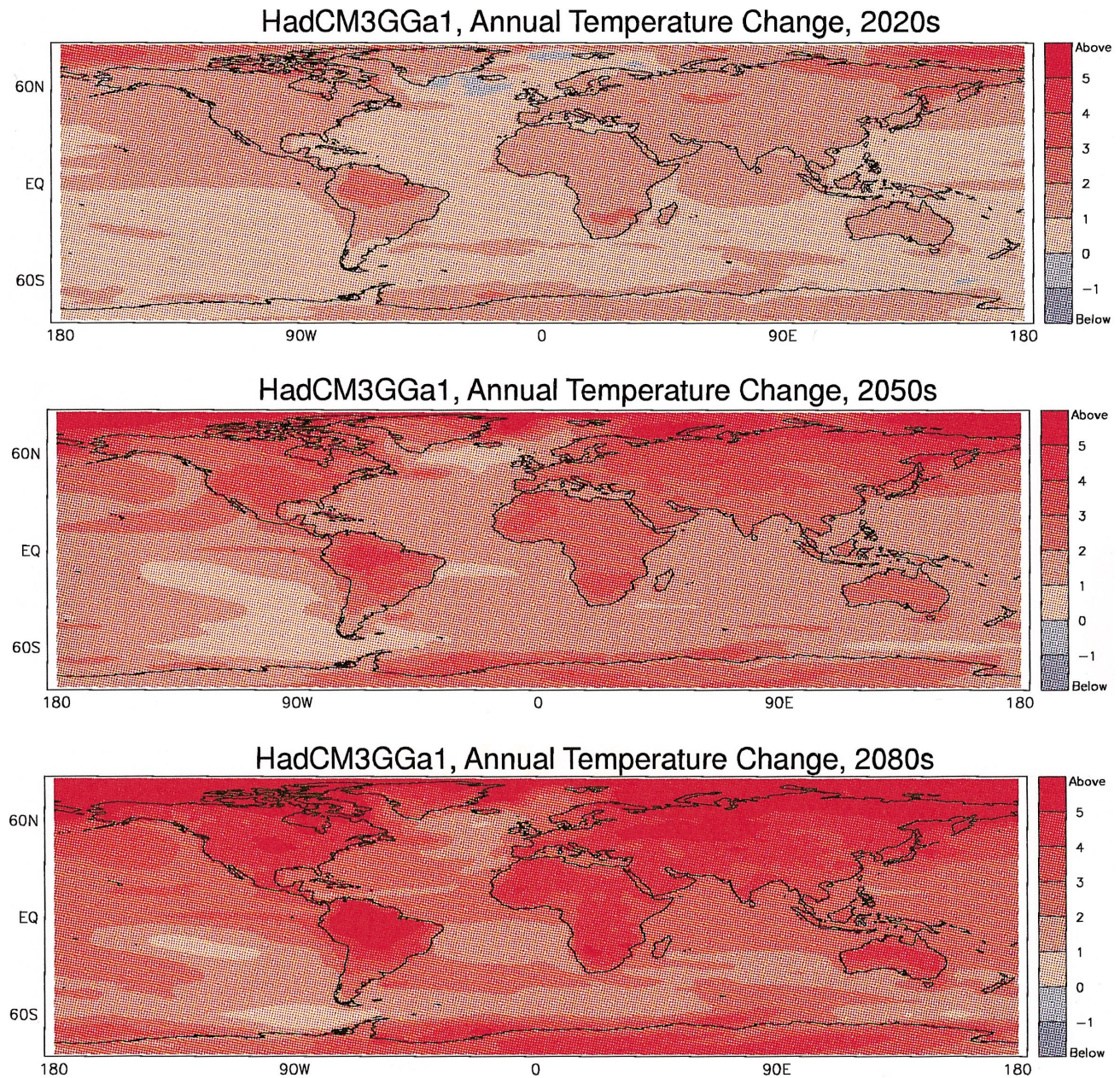


Fig. 5. As for Fig. 4, but for the one simulation using HadCM3.

In HadCM3, cloud cover increases in the southern extra-tropics and to a lesser extent in northern high latitudes. There are also increases in the equatorial Pacific and tropical southern Atlantic and Indian Oceans. There are large decreases in cloud cover over South America and the Caribbean, southern Africa and southern Europe. There is a closer relationship between increases in precipitation and increases in cloud in the tropics in this model than in HadCM2, perhaps because the changes generally represent shifts in the Inter-Tropical Convergence Zone as opposed to a local intensification of it (see Mitchell et al., 1998).

5.3. Changes in precipitation

The patterns of precipitation change during northern winter are quite similar between the two models (Fig. 7). Both show increases in precipitation in middle and high northern latitudes, little change in the sub-tropics, and more marked changes in the Inter-Tropical Convergence Zone. There are also some marked differences. HadCM3 tends to give larger areas of precipitation decrease in the tropics, especially over northern half of South America, whereas in HadCM2 there are substantial increases over parts of South America and equatorial Africa. In

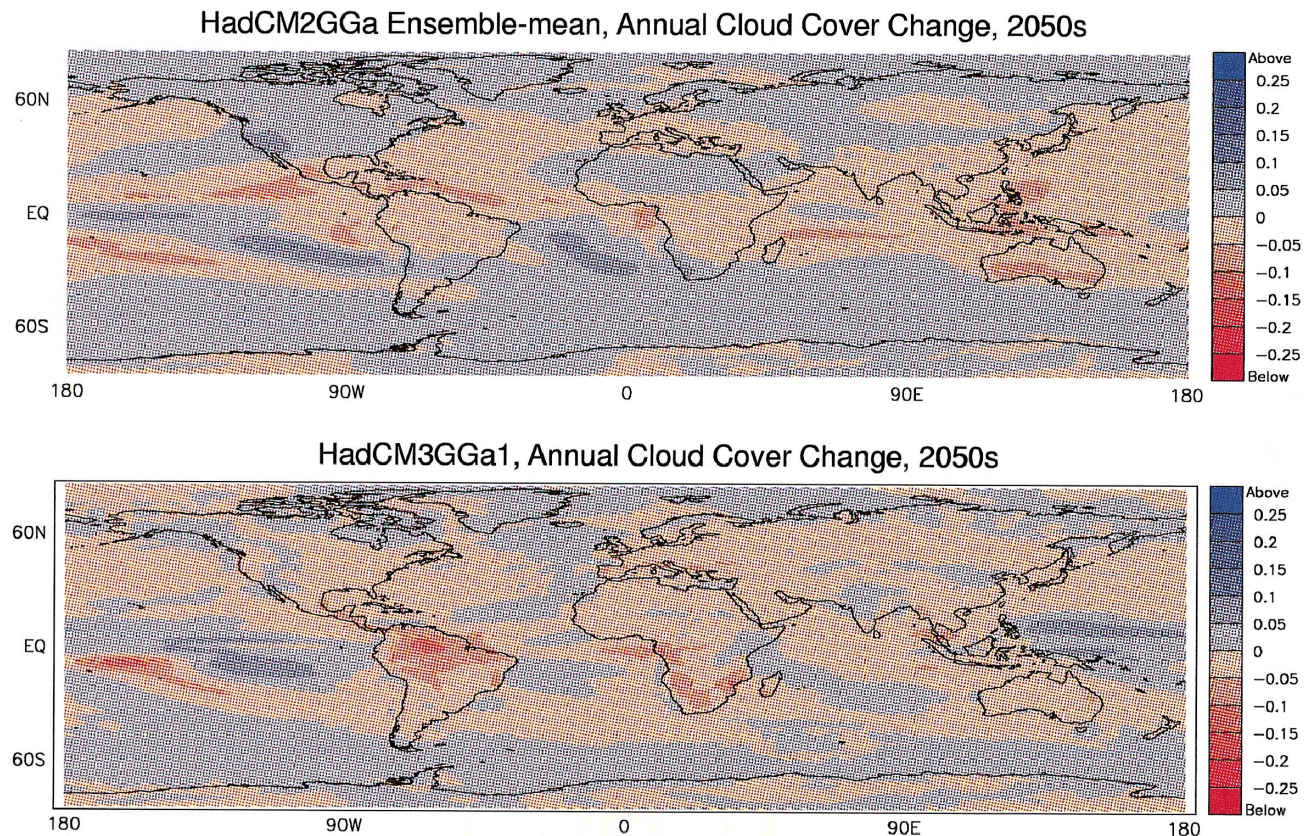


Fig. 6. Annual cloud cover change with respect to 1961–1990 for the 2050s for (top) HadCM2 ensemble-mean and (bottom) HadCM3.

HadCM2, there are also large precipitation increases in the northwest of North America, which replicate the precipitation anomalies observed during ENSO events when the tropical Pacific is unusually warm. This is probably due to the increase in tropical sea surface temperatures in HadCM2 (Fig. 4) which is absent in HadCM3 (Fig. 5).

In northern summer, there are some marked differences in the simulated precipitation changes over the northern mid-latitude continents (Fig. 7). Both models show reductions in precipitation over southern Europe, but in HadCM3 they are more marked and extend further east. HadCM2 produces increases over the United States, where HadCM3 produces decreases. Conversely, over India and eastern tropical Africa where HadCM2 produces decreases, the newer model produces increases. In general, HadCM3 produces larger precipitation increases over southeast Asia.

A certain amount of caution is advised when using the simulated changes in precipitation for impacts studies. The signal-to-noise ratio is much smaller for precipitation than for temperature. Thus, much of the detail in Fig. 7, especially for HadCM3, may arise from random climatic fluctuations and not from the increase in greenhouse gases. To illustrate this, we show the range of

precipitation changes by the 2050s in the four ensemble simulations carried out with HadCM2 (Fig. 8). In the main areas of precipitation, including the extra-tropical storm tracks and the sub-tropical summer monsoons over Brazil and southern Africa (Fig. 8) and to a lesser extent over southeast Asia and tropical Africa (Fig. 8), the intra-ensemble range is generally around 5%. However, over much of the tropics and sub-tropics, the range of precipitation changes exceeds 30% of the ensemble-mean. The regions of largest range include most of the major deserts and semi-arid regions. As a consequence, the regions that are potentially most vulnerable to reductions in precipitation are generally those where long-term trends are difficult to detect and where predictions tend to be less reliable because of the high level of natural precipitation variability.

Changes in regional precipitation are more sensitive to differences in model formulation than are differences in temperature. Certainly, there are large differences between the precipitation response to increases in greenhouse gases in different models (as between HadCM2 and HadCM3 and among the other models presented in Kattenberg et al., 1996). However, it is likely that some of the apparent discrepancy in the regional precipitation changes simulated by these different model experiments

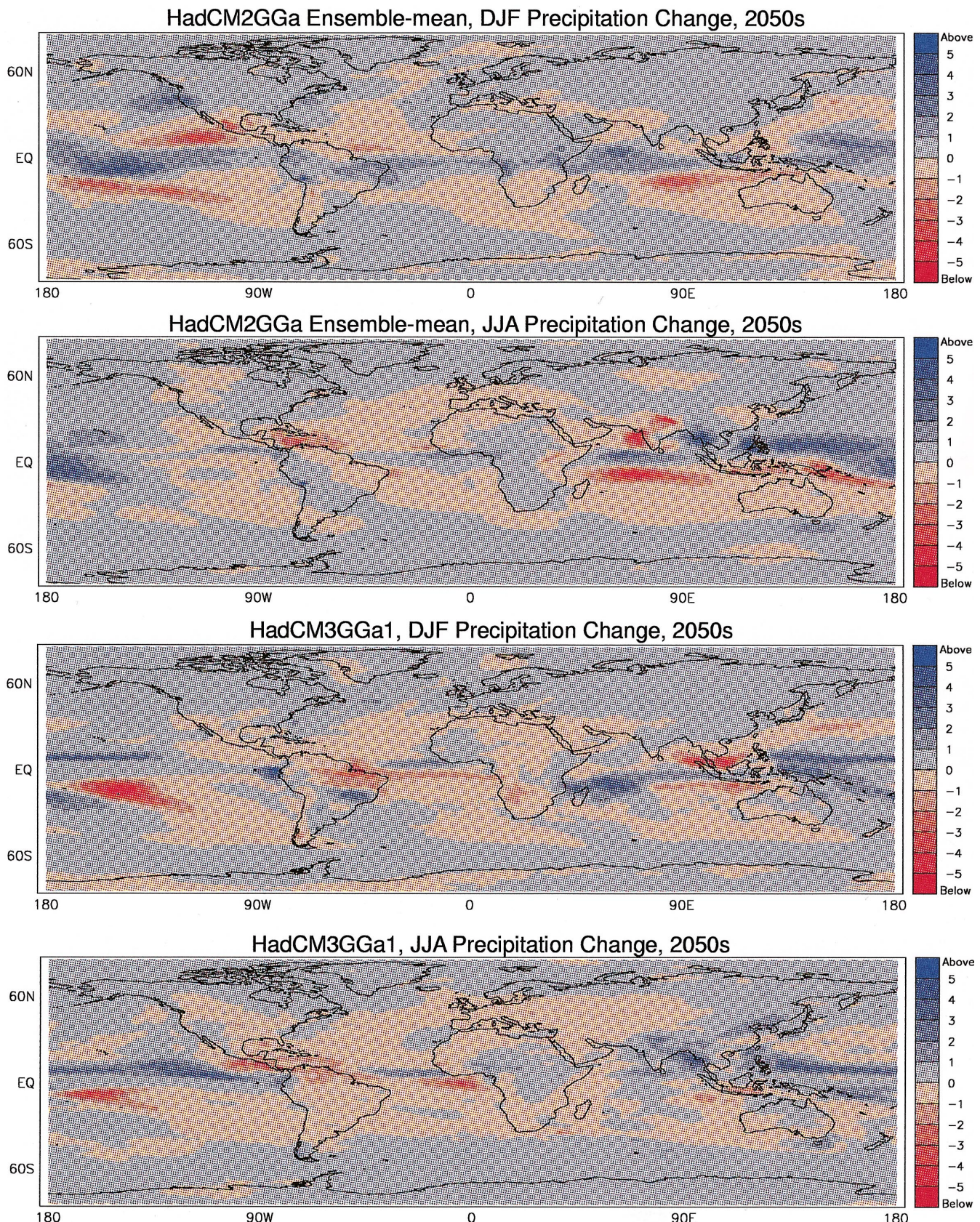


Fig. 7. Change in mean seasonal precipitation (mm/day) by the 2050s with respect to 1961–1990 for the HadCM2 ensemble-mean (top two panels; DJF and JJA) and for HadCM3 (bottom two panels; DJF and JJA).

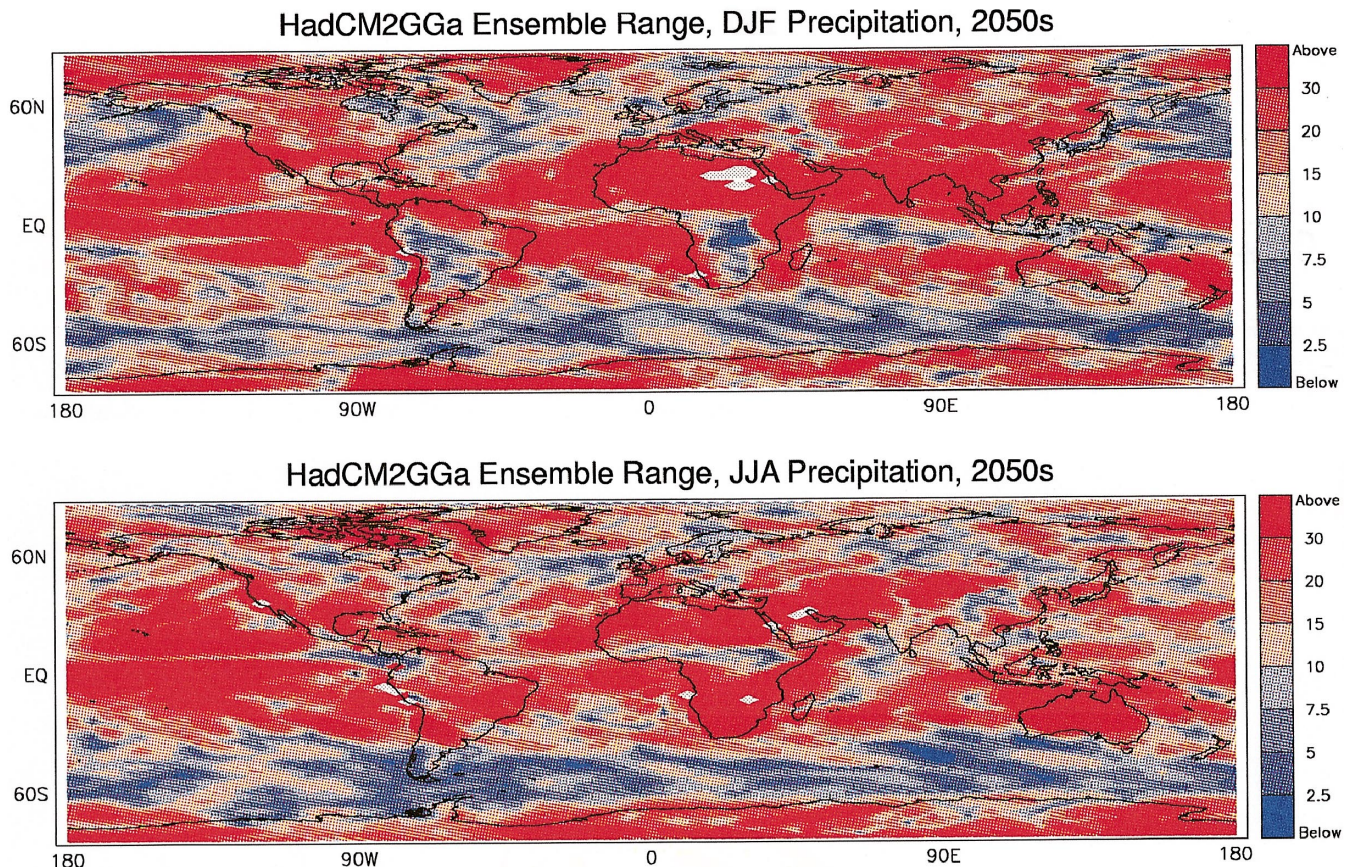


Fig. 8. The range of simulated mean seasonal precipitation changes (%) by the 2050s from the four ensemble members of the HadCM2 experiment; (top) DJF; (bottom) JJA.

is due to inadequate sampling of natural climate variability in regions where such internal variability is large. In summary, impact assessments based on simulated changes in precipitation need to be viewed with considerable caution.

6. Creating and applying the scenarios in impacts studies

The adopted baseline period for these scenarios was 1961–1990. All changes were calculated with respect to this period in the model perturbed simulations (i.e. t_1 in HadCM2GGa in Fig. 9). For the future we defined three 30-yr periods, those centred on 2025 (2010–2039), 2055 (2040–2069) and 2085 (2070–2099). As a form of shorthand these are referred to as the 2020, 2050 and 2080s.

While the impact models operate at a spatial resolution of 0.5° latitude/longitude, the same resolution as the observed 1961–1990 climatology, the GCM results existed at a resolution of 2.5° latitude by 3.75° longitude. To create the input climate data for the future time periods, the mean monthly GCM changes were added to the mean monthly observed climatology with no spatial interpolation of the GCM results. This approach means

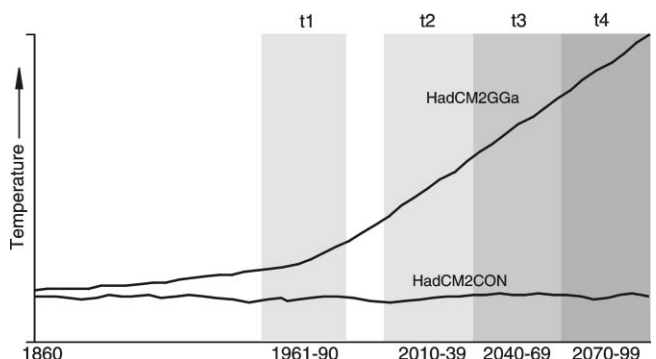


Fig. 9. Schematic representation of the time-slices used to define the climate change scenarios in the HadCM2 and HadCM3 experiments (see text for explanation).

that uniform GCM-derived scenario changes were applied to clusters of 35–40 0.5° cells on a GCM gridbox-by-gridbox basis. As a first-order approximation this may be a reasonable approach to take at a global-scale, although uncertainties related to downscaling of GCM results are not addressed using this method. Most of the impact models required mean temperature, precipitation,

vapour pressure and cloud cover, while some also required wind speed and diurnal temperature range. These variables were all reported by the HadCM2 and HadCM3 experiments. All changes were calculated in absolute rather than relative units. The ecosystem impacts group (White et al., 1999) used decadal-mean monthly climate values to create daily weather sequences using a stochastic weather generator built-in to their Hybrid ecosystem model.

The scenarios thus created are based on GCM simulations that excluded the effects of sulphate aerosols. This choice was made for a number of reasons. First, the IS92a sulphur dioxide (SO_2) forcing scenario used in the HadCM2 experiment assumed large increases in SO_2 emissions over the next century. More recent emissions scenarios (Nakicenovic et al., 1998), however, contain only a small rise in SO_2 emissions over the next couple of decades followed by reductions to levels lower than today's by 2100. Using patterns of climate change from GCM simulations forced by high sulphate aerosol concentrations would be inconsistent with new insights into sulphate aerosol loadings. Second, more recent sulphur cycle models generate a lower sulphate burden per tonne of sulphur dioxide emissions and the radiative effect of the sulphate particles in more sophisticated radiation models is smaller than previously calculated (Schimel et al., 1996; Haywood et al., 1997). Third, in addition to their direct effect, sulphate aerosols can also cool climate by changing the reflectivity and longevity of clouds. These indirect effects are now realised as being as at least as important as the direct effect, but were not included in the HadCM2 experiment. Above all, the short lifetime of sulphate particles in the atmosphere means that they can be seen as a temporary masking effect on the underlying warming trend due to greenhouse gases. For all these reasons, the scenarios described here are based on model simulations that only included the effects of greenhouse gas concentration increases.

7. Other scenario variables

7.1. Carbon dioxide concentrations

Actual atmospheric CO_2 concentrations were not specified for the HadCM2 experiment (see Section 4 above) and so they have to be estimated using some assumed relationship between CO_2 forcing and total greenhouse gas forcing. For the estimates used in the impacts studies reported in this Special Issue, we used a relationship consistent with emissions scenarios SA90 as reported in IPCC (1990). These only differ by ± 25 ppmv from concentrations for HadCM2 estimated using alternative relationships. For HadCM3, CO_2 concentrations were specified to replicate those reported by IPCC in 1996 (Kattenberg et al., 1996) for the IS92a emissions scenario.

Table 1

Summary global-mean changes with respect to 1961–90 for the 30-yr periods centred on 2020s, 2050s and 2080s for the scenario based on HadCM2 (ensemble-mean) and on HadCM3. 'Best guess' values for the IS92a emissions scenario, with no aerosol forcing, calculated by the IPCC (Kattenberg et al., 1996) are also shown

	1961–90	2020s	2050s	2080s
IS92a				
Temperature change (K)	0	1.0	1.7	2.4
Sea-level rise (cm)	0	20	38	58
CO_2 (ppmv)	334	434	528	638
HadCM2				
Temperature change (K)	0	1.2	2.1	3.1
Precipitation change (%)	0	1.6	2.9	4.5
Sea-level rise (cm)	0	12	25	41
CO_2 (ppmv)	334	441	565	731
HadCM3				
Temperature change (K)	0	1.1	2.1	3.0
Precipitation change (%)	0	1.3	2.4	3.2
Sea-level rise (cm)	0	12	24	40
CO_2 (ppmv)	334	433	527	642

Relative to 1961–1990, CO_2 concentrations increase by the 2080s by 119% for HadCM2 and by 92% for HadCM3. The concentrations for the three future time periods are listed in Table 1, along with other summary indicators of the climate change scenarios. Estimates of these indicators for the IS92a emissions scenario reported by IPCC in 1996 are shown for comparison.

7.2. Socio-economic assumptions

The climate scenarios described in Sections 5 and 6 contain no information about the accompanying changes in the state of the world. Such changes can have profound effects on environmental indicators and their effects must also be assessed alongside climate change (Parry and Carter, 1998). For the series of impact studies reported in this Special Issue we made the following assumptions.

The forcing scenario used to drive the GCM experiments approximated a 1% per annum compounded growth in atmospheric greenhouse gas concentration from 1990 to 2100. This forcing scenario quite closely approximates the greenhouse gas forcing that results when the IS92a emissions scenario is converted into an equivalent- CO_2 radiative forcing using equations reported in the IPCC 1996 (Kattenberg et al., 1996). Given this approximation, we adopted basic socio-economic assumptions that were consistent with the IS92a emissions scenario and which were based on World Bank and EMF14 estimates (Bos et al., 1994; Energy Modelling Forum, 1995). These data are summarised in Table 2. Other assumptions used in specific impacts assessments (e.g. water resources, Arnell, 1999) were developed

further, but were consistent with these aggregate global scenarios.

7.3. Sea-level change

The simulated rise in global-mean sea-level due to thermal expansion and glacier melt reaches about 0.5 m in both models by 2100 (Table 1). The rise by 2100 is about 10% larger in HadCM2 than in HadCM3 (Fig. 10). Note the acceleration in the rate of sea-level rise over the 21st century. This is two to four times the estimated observed rate of increase during the 20th century (Warrick et al., 1996). Note also that even if greenhouse gas concentrations were to be stabilised at their 2100 levels, sea-level would continue to rise for several centuries because of thermal expansion as the deep ocean temperature slowly warmed to reach its new equilibrium.

Table 2
Population and GDP assumptions used for the non-climatic scenarios

	1990	2020s	2050s	2080s
Population (billions)	5.3	8.1	9.8	10.7
GDP (trillion 1990 \$)	20.1	54.7	104.4	188.9
GDP/capita (thousand 1990 \$)	3.8	6.8	10.7	17.7

7.4. Nitrogen deposition

The ecosystem model Hybrid (White et al., 1999) is driven by patterns of mineral nitrogen inputs to the soil, in addition to climate and atmospheric CO₂ change. This nitrogen input is attained by summing the biological nitrogen fixation — assumed to be 10 kg N ha⁻¹ yr⁻¹ in all model grid cells (Friend and White, 1999) — and the atmospheric nitrogen deposition each year. Atmospheric nitrogen deposition for each grid cell was derived from NH_x and NO_y deposition estimates for pre-industrial, current (1961–1990) and 2050 conditions (Holland et al., 1997; Dentener, pers. comm.), assuming an exponential increase with time.

8. Uncertainties and discussion

The climate change scenarios created here are based on one future forcing scenario, namely a ~1% per annum growth in CO₂ equivalent concentration, and on results from successive versions of a global climate model from just one modelling centre, namely the Hadley Centre. Clearly, there are alternative forcing futures which may be equally plausible to the one used here. IPCC in 1992 (Leggett et al., 1992) published six alternative emissions scenarios and more recently the IPCC through the Special Report on Emissions Scenarios

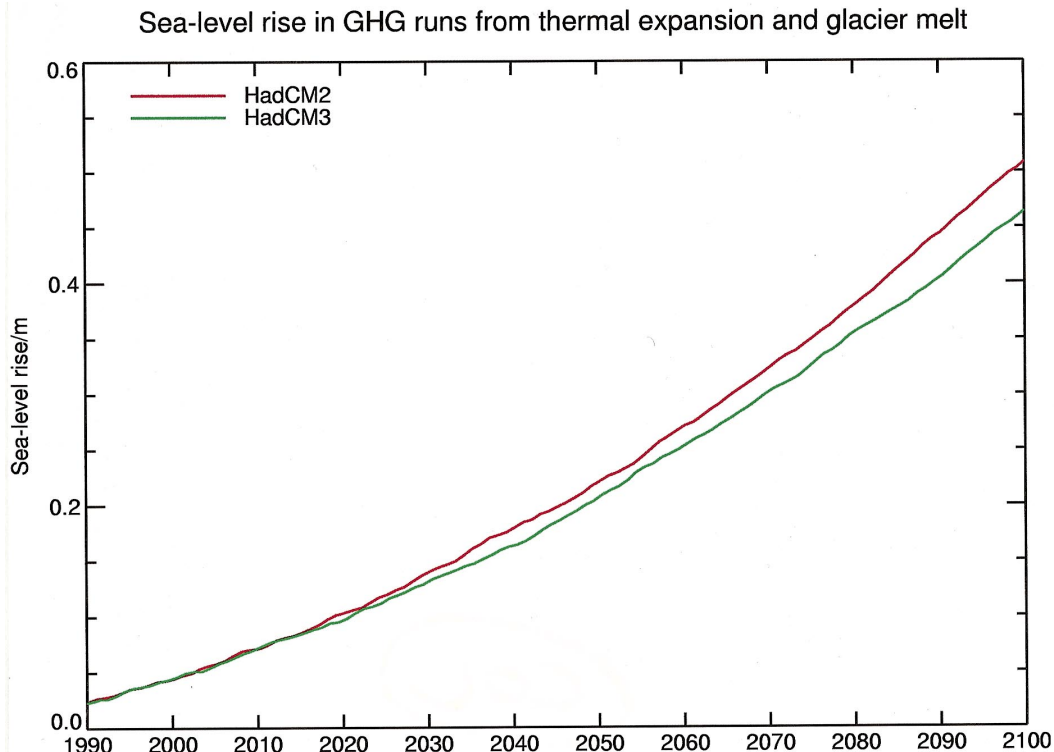


Fig. 10. Increase in global-mean sea-level with respect to 1961–1990 due to thermal expansion and glacier melt for the HadCM2 ensemble-mean (red line) and HadCM3 (green line) experiments.

(SRES) working group are publishing four new emissions scenarios (Nakicenovic et al., 2000). The range of future forcing trajectories in the new SRES scenarios is from about 0.5% per annum growth in greenhouse gas concentration to about 1.1% per annum growth. The greenhouse gas forcing scenario used here is therefore towards the higher end of this range. If a forcing scenario of only 0.5% per annum growth had been used to create our climate scenarios, the global warming would have been between 30 and 40% less than simulated for our scenarios (Mitchell et al., 1999). If, however, we had been considering scenarios including the effects of sulphate aerosols, then the reduced aerosol forcing in the SRES scenarios compared to IS92 scenarios would have partly compensated for lower greenhouse gas forcing, at least at the global-mean scale.

The climate sensitivity is another major source of uncertainty in future climate prediction. The sensitivities over the next century of the two model versions used here are about 2.5 and 3.3°C. These values are quite representative of those calculated using other GCMs (cf. Kattenberg et al., 1996) and fall in the middle of the full IPCC range of 1.5–4.5°C. Again, however, a full risk assessment of future climate change impacts should consider climate scenarios associated with climate sensitivities lower and higher than these Hadley Centre estimates. It should also be noted that GCMs may produce different regional patterns of climate response even if the forcing and the global-mean sensitivity are the same.

We have not used results from experiments in which the effects of other anthropogenic factors, in particular sulphate aerosols are simulated alongside those of greenhouse gases. Our reasons for this were quite deliberate (see Section 6), although we recognise that for at least some regions and for some decades into the future these effects may be important. Future GCM climate change

experiments will use more realistic SO₂ emissions scenarios (Nakicenovic et al., 2000) and will include the indirect as well as the direct effect of sulphate aerosol concentration changes.

The non-linearity of the climate system limits the degree to which climate is predictable. Thus, predictions for the future are sensitive to small changes in the initial ocean–atmosphere conditions at which anthropogenic forcing is introduced (Cubasch et al., 1994; Mitchell et al., 1999). This sensitivity can be explored through the use of ensemble simulations as done here with the HadCM2 experiment. Impacts assessments based on impact simulations made using four ensemble scenarios should provide more robust estimates of the effects of climate change than an impact assessment made using just a single-model realisation. In this regard, the anthropogenic component of the impact responses based on the HadCM3 scenario is likely to be less well defined than those based on the four member HadCM2 ensemble (cf. Hulme et al., 1999). Impacts results based on the single HadCM3 simulation in particular, should be cautiously interpreted because of the signal-to-noise ratios in both the climate change and the impacts responses are lower than in the HadCM2 ensemble.

Different GCMs yield different regional patterns of climate change, even when forced by the same scenario (Kittel et al., 1998). Some of these differences may be due to different climate sensitivities and some may be due to climate system unpredictability as summarised above. However, some of the differences are a reflection of fundamental differences in model design, which in turn are a function of incomplete understanding/parameterisation of important physical processes and feedbacks. We illustrate this point in Fig. 11 which shows inter-model differences in the regional climate response of the Amazon Basin to greenhouse gas forcing for the 2050s and

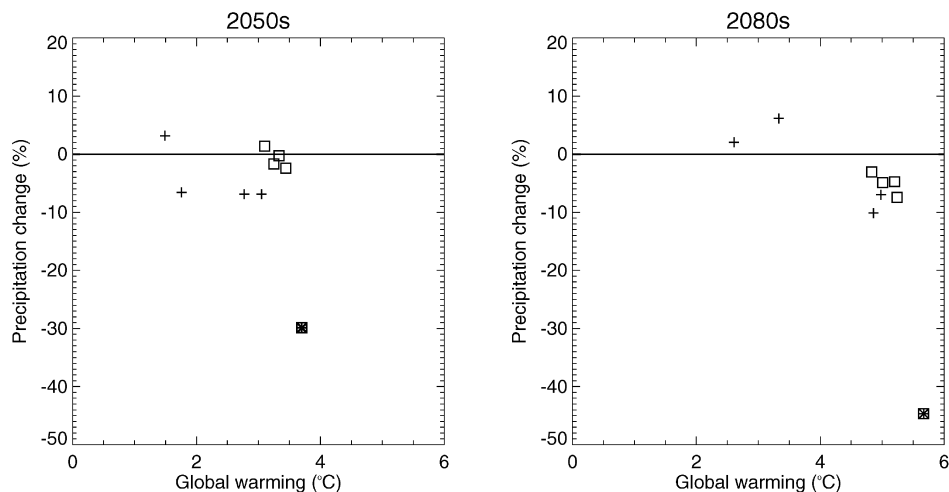


Fig. 11. Change in annual-mean temperature and precipitation for the Amazon (35–65°W, 5°N–10°S) with respect to 1961–1990 for the 2050s (left) and 2080s (right). Changes are extracted for the HadCM2 ensemble (open squares) and HadCM3 simulation (filled square) used in this paper, and also for four independent GCM experiments (crosses), results from which are available from the IPCC Data Distribution Centre (DDC, 1999).

2080s. The large drying over this region in the HadCM3 simulation (cf. Fig. 7) is not reproduced in other GCMs, at least two of which yield much smaller warming rates over the Amazon than either HadCM2 or HadCM3 (Fig. 11). These inter-model differences in regional response should be reflected in a full risk assessment of climate change impacts.

Finally, we point out that the climate change scenarios created here, and applied to impact studies reported in this Special Issue, contain changes only in mean monthly climate. We did not provide estimates of changes in inter-annual or inter-daily climate variability, changes which potentially can have a large influence on the simulation of a climate change indicator (e.g. Mearns et al., 1997).

All of the above limitations should be recognised when interpreting the results of the impacts studies that make use of the climate change scenarios described here. A full risk assessment of climate change impact would attempt to sample the various sources of uncertainty mentioned above in a more comprehensive manner (Walsh et al., 1998; Hulme and Carter, 1999).

Acknowledgements

The HadCM2 and HadCM3 experiments were supported by the UK Department of Environment, Transport and the Regions (DETR) under Contract PECD/7/12/37. JFBM, TCJ, WJI and JAL are supported by the Public Meteorological Service Research and Development programme. MH is supported by the DETR under Contract EPG 1/1/85. We thank Jonathan Gregory for producing the changes in sea-level and Ruth Doherty for producing Fig. 11. The processing and distribution of the GCM results was undertaken by the Climate Impacts LINK Project (UK DETR Contract EPG 1/1/68). The observed global climatology has been constructed by the Climatic Research Unit with support from, among others, the NERC (Grant No. GR3/09721).

References

- Airey, M.J., Hulme, M., Johns, T.C., 1996. Evaluation of simulations of terrestrial precipitation by the UK Met Office/Hadley Centre model. *Geophysical Research Letters* 23, 1657–1660.
- Arnell, N.W., 1999. Climate change and global water resources. *Global Environmental Change* 9, S31–S49.
- Bos, E., Vu, M.T., Massiah, E., Bulatao, R.A., 1994. World Population Projections 1994–95: Estimates and Projections with Related Demographic Statistics. In: World Bank. The Johns Hopkins University Press, New York, USA.
- Bryan, K., 1969a. A numerical model for the study of the circulation of the world ocean. *Journal of Computational Physics* 3, 347–376.
- Bryan, K., 1969b. Climate and the ocean circulation. III The ocean model. *Monthly Weather Review* 97, 806–827.
- Carnell, R.E., Senior, C.A., 1998. Changes in mid-latitude variability due to increasing greenhouse gases and sulphate aerosols. *Climate Dynamics* 14, 369–383.
- Cattle, H., Crossley, J., 1995. Modelling Arctic climate change. *Philosophical Transactions of the Royal Society of London A* 352, 201–213.
- Cox, M.D., 1984. A primitive equation, three-dimensional model of the ocean. *GFDL Ocean Group Technical Report No.1*, Princeton NJ, USA, 143pp.
- Cox, P., Betts, R., Bunton, C., Essery, R., Rowntree, P.R., Smith, J., 1998. The impact of new land surface physics on the GCM simulation of climate and climate sensitivity. *Climate Dynamics*, in press.
- Cubasch, U., Santer, B.D., Hellbach, A., Hegerl, G., Höck, H., Maier-Reimer, E., Mikolajewicz, U., Stössel, A., Voss, R., 1994. Monte Carlo climate change forecasts with a coupled ocean-atmosphere model. *Climate Dynamics* 10, 1–19.
- Cusack, S., Slingo, A., Edwards, J.M., Wild, M., 1998. The radiative impact of a simple aerosol climatology on the Hadley Centre Atmospheric GCM. *Quarterly Journal of the Royal Meteorological Society*, in press.
- DDC, 1999. The IPCC Data Distribution Centre Web site: http://ipcc-ddc.cru.uea.ac.uk/cru_data/cru_index.html.
- Dolman, A.J., Gregory, D., 1992. The parameterisation of rainfall interception in GCMs. *Quarterly Journal of the Royal Meteorological Society* 118, 455–467.
- Edwards, J.M., Slingo, A., 1996. Studies with a flexible new radiation code. I: choosing a configuration for a large-scale model. *Quarterly Journal of Royal Meteorological Society* 122, 689–719.
- Emanuel, W.R., Shugart, H.H., Stevenson, M.P., 1985. Climatic change and the broad-scale distribution of terrestrial ecosystem complexes. *Climatic Change* 7, 29–43.
- Energy Modelling Forum, 1995. Second round study design for EMF 14: integrated assessment of global climate change. Energy Modeling Forum Working Paper No. 14.1, March.
- Friend, A.D., White, A., 1999. Evaluation and analysis of a dynamic terrestrial ecosystem model under pre-industrial conditions at the global scale. *Global Biogeochemical Cycles*, in press.
- Gates, W.L., Nelson, R.B., 1973. A new tabulation of the Scripps topography on a 1 degree global grid Part II: ocean depths. Santa Monica, California, Rand Corp. Contract no. DAHC15-73-0181.
- Gent, P., McWilliams, J.C., 1990. Isopycnal mixing in ocean circulation models. *Journal of Physical Oceanography* 20, 150–155.
- Giorgi, F., Francisco, R., 1999. On the predictability of regional climate change. *Climate Dynamics*, submitted for publication.
- Gordon, C., Cooper, C., Senior, C., Banks, H., Gregory, J.M., Johns, T.C., Mitchell, J.F.B., Wood, R., 1999. Simulation of SST, sea-ice extents and ocean heat transports in a coupled model without flux adjustments. *Climate Dynamics*, in press.
- Gregory, D., Allen, S., 1991. The effect of convective scale down-draughts upon NWP and climate simulations. 9th Conference on Numerical Weather Prediction, Amer. Meteor. Soc., Denver, USA, pp. 122–123.
- Gregory, D., Kershaw, R., Inness, P.M., 1997. Parameterisation of momentum transport by convection II: tests in single column and general circulation models. *Quarterly Journal of Royal Meteorological Society* 123, 1153–1183.
- Gregory, D., Rowntree, P.R., 1990. A mass flux convection scheme with representation of ensemble characteristics and stability dependent closure. *Monthly Weather Review* 118, 1483–1506.
- Gregory, D., Shutts, G.J., Mitchell, J.R., 1998. A new gravity wave drag scheme incorporating anisotropic orography and low level wave breaking: impact upon the climate of the UK Meteorological Office Unified Model. *Quarterly Journal of the Royal Meteorological Society* 124, 463–493.
- Gregory, J.M., Mitchell, J.F.B., 1997. The climate response to CO₂ of the Hadley Centre coupled AOGCM with and without flux adjustment. *Geophysical Research Letters* 24, 1943–1946.

- Haywood, J.M., Roberts, D.L., Slingo, A., Edwards, J.M., Shine, K.P., 1997. General circulation model calculations of the direct radiative forcing by anthropogenic sulfate and fossil fuel soot aerosol. *Journal of Climate* 10, 1562–1577.
- Hibler, W.D., 1979. A dynamic-thermodynamic sea-ice model. *Journal of Physical Oceanography* 9, 815–846.
- Holland, E.A., Braswell, B.H., Lamarque, J.F. et al., 1997. Variations in the predicted spatial distribution of atmospheric nitrogen deposition and their impact on carbon uptake by terrestrial ecosystems. *Journal of Geophysical Research* 102, 15,849–15,866.
- Hulme, M., Carter, T.R., 1999. Representing uncertainty in climate change scenarios and impact studies. *ECLAT-2 Workshop Report*, CRU, Norwich, in press.
- Hulme, M., Barrow, E.M., Arnell, N., Harrison, P.A., Downing, T.E., Johns, T.C., 1999. Relative impacts of human-induced climate change and natural climate variability. *Nature* 397, 688–691.
- IPCC, 1990. In: Houghton, J.T., Jenkins, G.J., Ephraums, J.J. (Eds.), *Climate Change: The IPCC Scientific Assessment*. Cambridge University Press, Cambridge, UK, 364pp.
- Johns, T.C., Carnell, R.E., Crossley, J.F., Gregory, J.M., Mitchell, J.F.B., Senior, C.A., Tett, S.F.B., Wood, R.A., 1997. The second Hadley Centre coupled ocean-atmosphere GCM: model description, spin-up and validation. *Climate Dynamics* 13, 103–134.
- Kattenberg, A., Giorgi, F., Grassl, H., Meehl, G.A., Mitchell, J.F.B., Stouffer, R.J., Tokioka, T., Weaver, A.J., Wigley, T.M.L., 1996. Climate models — projections of future climate. In: Houghton, J.T., Meiro Filho, L.G., Callendar, B.A., Harris, N., Kattenburg, A., Maskell, K. (Eds.), *Climate Change 1995: the science of climate change change*. Cambridge University Press, Cambridge, UK, pp. 285–358.
- Kittel, T.G.F., Giorgi, F., Meehl, G.A., 1998. Intercomparison of regional biases and doubled CO₂-sensitivity of coupled atmosphere-ocean general circulation model experiments. *Climate Dynamics* 14, 1–15.
- Kraus, E.B., Turner, J.S., 1967. A one dimensional model of the seasonal thermocline. Part II. *Tellus* 19, 98–105.
- Leggett, J., Pepper, W.J., Swart, R.J., 1992. Emissions scenarios for the IPCC: an update. In: Houghton, J.T., Callander, B.A., Varney, S.K. (Eds.), *Climate change 1992: the supplementary report to the IPCC scientific assessment*. Cambridge University Press, Cambridge, pp. 75–95.
- Martens, W.J.M., Kovats, S., Nijhof, S., de Vries, P., Livermore, M., McMichael, A.J., Bradley, D., Cox, J., 1999. Climate change and future populations at risk of malaria. *Global Environmental Change*, this issue.
- Martin, G.M., Johnson, D.W., Spice, A., 1994. The measurement and parameterisation of effective radius of droplets in warm stratocumulus clouds. *Journal of Atmospheric Science* 51, 1823–1842.
- Mearns, L.O., Rosenzweig, C., Goldberg, R., 1997. Mean and variance change in climate scenarios: methods, agricultural applications, and measures of uncertainty. *Climatic Change* 35, 367–396.
- Milton, S.F., Wilson, C.A., 1996. The impact of parameterised sub-grid scale orographic forcing on systematic errors in a global NWP model. *Monthly Weather Review* 124, 2023–2045.
- Mitchell, J.F.B., Johns, T.C., Senior, C.A., 1998. Transient response to increasing greenhouse gases using models with and without flux adjustment. *Hadley Centre Technical Note No.2*, Hadley Centre, UK Meteorological Office, UK, 13pp. + xxi.
- Mitchell, J.F.B., Gregory, J.M., 1992. Climatic consequences of emissions and a comparison of IS92a and SA90. In: Houghton, J.T., Callander, B.A., Varney, S.K. (Eds.), *Climate Change 1992: The Supplementary Report to the IPCC Scientific Assessment*. Cambridge University Press, Cambridge, pp. 171–175.
- Mitchell, J.F.B., Johns, T.C., 1997. On the modification of global warming by sulphate aerosols. *Journal of Climate* 10, 245–267.
- Mitchell, J.F.B., Johns, T.C., Eagles, M., Ingram, W.J., Davies, R.A., 1999. Towards the development of climate change scenarios. *Climatic Change* 41, 547–581.
- Mitchell, J.F.B., Johns, T.C., Gregory, J.M., Tett, S.F.B., 1995. Climate response to increasing levels of greenhouse gases and sulphate aerosols. *Nature* 376, 501–504.
- Nakicenovic, N. et al., 2000. Special Report on Emissions Scenarios. Intergovernmental Panel on Climate Change, under review.
- Nakicenovic, N., Grubler, A., McDonald, A. (Eds.), 1998. *Global Energy Perspectives*. Cambridge University Press, Cambridge, MA, 299pp.
- New, M., Hulme, M., Jones, P.D., 1999a. Representing twentieth century space-time climate variability. Part 1: development of a 1961–1990 mean monthly terrestrial climatology. *Journal of Climate* 12, 829–856.
- New, M., Hulme, M., Jones, P.D., 1999b. Representing twentieth century space-time climate variability. Part 2: development of 1901–1996 monthly grids of terrestrial surface climate. *Journal of Climate*, in press.
- Nicholls, R.J., Hoozemans, F., Marchand, M., 1999. Increasing flood risk and wetland losses due to global sea-level rise: regional and global analyses. *Global Environmental Change*, this issue.
- Palmer, T.N., Shutts, G.J., Swinbank, R., 1986. Alleviation of a systematic westerly bias in general circulation and numerical weather prediction models through an orographic gravity wave drag parameterisation. *Quarterly Journal of the Royal Meteorological Society* 112, 1001–1039.
- Parry, M.L., Carter, T., 1998. *Climate Impact and Adaptation Assessment*. Earthscan, London, 176pp.
- Parry, M.L., Rosenzweig, C., Iglesias, A., Fischer, G., Livermore, M.T.J., 1999. Climate change and world food security: a new assessment. *Global Environmental Change* 9, S51–S67.
- Pope, V.D., Gallani, M.L., Rowntree, P.R., Stratton, R.A., 1999. The impact of new physical parametrizations in the Hadley Centre climate model – HadAM3. *Climate Dynamics*, submitted for publication.
- Roether, W., Roussenov, V.M., Well, R., 1994. A tracer study of the thermohaline circulation of the eastern Mediterranean. In: Malanotte-Rizzoli, P., Robinson, A.R. (Eds.), *Ocean Processes in Climate Dynamics: Global and Mediterranean Example*. Kluwer Academic Press, Germany, pp. 371–394.
- Rosenzweig, C., 1985. Potential CO₂-induced climate effects on North American wheat-producing regions. *Climatic Change* 4, 239–254.
- Santer, B.D., 1985. The use of general circulation models in climate impact analysis – a preliminary study of the impacts of CO₂-induced climate change on West European agriculture. *Climatic Change* 7, 71–93.
- Schimel, D., et al., 1996. Radiative forcing of climate change. In: Houghton, J.T., Meiro Filho, L.G., Callendar, B.A., Kattenburg, A., Maskell, K. (Eds.), *Climate Change 1995: the Science of Climate Change*. Cambridge University Press, Cambridge, UK, pp. 65–131.
- Semtner, A.J., 1976. A model for the thermodynamic growth of sea ice in numerical investigations of climate. *Journal of Physical Oceanography* 6, 379–389.
- Slingo, A., 1989. A GCM parameterisation for the shortwave radiative properties of water clouds. *Journal of Atmospheric Science* 46, 1419–1427.
- Slingo, A., Wilderspin, R.C., 1986. Development of a revised longwave radiation scheme for an atmospheric general circulation model. *Quarterly Journal of Royal Meteorological Society* 112, 371–386.
- Smith, R.N.B., 1990. A scheme for predicting layer clouds and their water content in a general circulation model. *Quarterly Journal of Royal Meteorological Society* 116, 435–460.
- Smith, R.N.B., 1993. Experience and developments with the layer cloud and boundary layer mixing schemes in the UK Meteorological Office Unified Model. Proceedings of the ECMWF/GCSS Workshop on Parameterisation of the Cloud-Topped Boundary Layer, 8–11 June, 1993, ECMWF, Reading, UK.
- Tett, S.F.B., Johns, T.C., Mitchell, J.F.B., 1997. Global and regional variability in a coupled AOGCM. *Climate Dynamics* 31, 303–324.

- Visbeck, M., Marshall, J., Haine, T., Spall, M., 1997. On the specification of eddy transfer coefficients in coarse resolution ocean circulation models. *Journal of Physical Oceanography* 27, 381–402.
- Walsh, K.J., Allan, R.J., Jones, R.N., Pittock, A.B., Suppiah, R., Whetton, P.H., 1998. Climate change in Queensland under enhanced greenhouse conditions: first annual report. CSIRO Research Report to the Queensland State Government, Mordialloc, Australia, 84pp.
- Warrick, R.A., Le Provost, C., Meier, M.F., Oerlemans, J., Woodworth, P.L., 1996. Changes in sea-level. In: Houghton, J.T., Meiro Filho, L.G., Callendar, B.A., Kattenburg, A., Maskell, K. (Eds.), *Climate Change 1995: The Science of Climate Change*. Cambridge University Press, Cambridge, UK, pp. 359–405.
- Warrilow, D.A., Sangster, A.B., Slingo, A., 1986. Modelling of land surface processes and their influence on European climate. Met O 20 Dynamical Climatology Technical Note 38, Meteorological Office, Bracknell, UK.
- White, A., Cannell, M.G.R., Friend, A.D., 1999. Climate change impacts on ecosystems and the terrestrial carbon sink: a new assessment. *Global Environmental Change*, this issue.
- Wood, R.A., Keen, A.B., Mitchell, J.F.B., Gregory, J.M., 1999. Spatial variations in the stability of the North Atlantic thermohaline circulation under greenhouse gas forcing. *Nature* 399, 572–575.